Surface Properties of a Series of Amphiphilic Dendrimers with Short Hydrophobic Chains

ARTICLE *in* LANGMUIR · APRIL 2008

Impact Factor: 4.46 · DOI: 10.1021/la7021177 · Source: PubMed

6 AUTHORS, INCLUDING:

Jirun Sun
American Dental Association
37 PUBLICATIONS **203** CITATIONS
SEE PROFILE

Muruganathan Ramanathan
Oak Ridge National Laboratory
29 PUBLICATIONS **453** CITATIONS
SEE PROFILE

George Richard Newkome
University of Akron
499 PUBLICATIONS **12,767** CITATIONS
SEE PROFILE

Paul Russo
Georgia Institute of Technology
131 PUBLICATIONS **2,299** CITATIONS
SEE PROFILE

Surface Properties of a Series of Amphiphilic Dendrimers with Short Hydrophobic Chains

Jirun Sun,[†] Muruganathan Ramanathan,[‡] Derek Dorman,[†] George R. Newkome,[§] Charles N. Moorefield,[§] and Paul S. Russo*,[†]

Department of Chemistry and Macromolecular Studies Group, Louisiana State University, Baton Rouge, Louisiana 70803, Department of Chemistry and Biochemistry, Florida State University, Tallahassee, Florida 32306, and Departments of Chemistry and Polymer Science, The University of Akron, Akron, Ohio 44325-4717

Received July 16, 2007

A series of tree-shaped, amphiphilic dendrimers was synthesized. The products belong to the family of one-directional arborols of the form ([9]-*n*), where the notation signifies that each molecule has nine hydroxyl groups ([9]-) as the hydrophilic head and an alkyl chain as the hydrophobic moiety ($n = 6$, 8, or 10 carbon atoms). The surfactant character changes dramatically as the number of methylene groups increases. The critical micelle concentration of [9]-6 was determined, and pressure−area isotherms of the less soluble [9]-8 and [9]-10 were obtained. Large structures existed atop the spread layers. Large structures were also found in solutions of [9]-6.

Introduction

Micellar aggregates formed by amphiphilic molecules above their critical micelle concentration (cmc)[1−3] are of interest in drug delivery and biomimetic applications.[4−9] One challenge in such systems is to form stable micelles using amphiphilic molecules whose hydrophobic chains have less than 10 carbon atoms. This study tested the hypothesis that molecules having large hydrophilic headgroups attached to stubby aliphatic chains might be effective. One-directional arborols[10−12] ([9]-*n*) are tree-shaped amphiphilic dendrimers with nine hydroxyl groups ([9]-) as the hydrophilic head and an alkyl chain as the hydrophobic moiety (*n* stands for the number of carbons in the alkyl chain). In this work, $n = 6$, 8, or 10; thus, three one-directional arborols, [9]-10, [9]-8, and [9]-6, are described. Potential applications of these molecules are deferred to the conclusion, but other amphiphilic dendrimers have been designed for applications such as gene delivery[13] or multipurpose superstructures.[14]

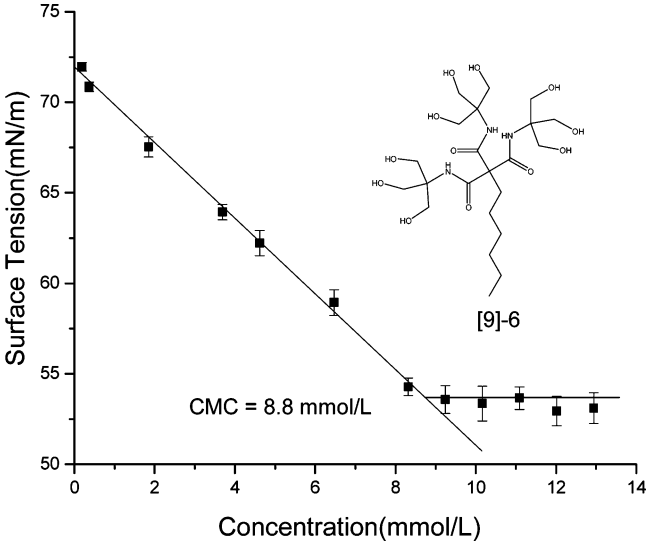

Figure 1. Surface tension of [9]-6. Inset: structure of the one-directional arborol [9]-6.

Materials and Methods

Synthesis of One-Directional Arborols. Scheme 1 is representative. The detailed synthesis follows the procedures developed to produce two-directional arborols by Newkome et al.;[10,12] see also the synthesis of a [27]-*n* arborol.[11]

Alkylation of Triethyl Methanetricarboxylate. General Procedure. The appropriate bromoalkane (15 mmol) was added to a stirred solution of $NaC(CO_2Et)_3$ (17 mmol) in *N*,*N*-dimethylformamide (DMF, 20 mL) at 90 °C. After 12 h, the solution was cooled, and toluene (100 mL) was added. This solution was washed with saturated $NaHCO_3$ (4 × 100 mL), then dried over ($MgSO_4$),

* To whom correspondence should be addressed. E-mail: chruss@lsu.edu.
† Louisiana State University.
‡ Florida State University.
§ The University of Akron.

(1) Kellermann, M.; Bauer, W.; Hirsch, A.; Schade, B.; Ludwig, K.; Bottcher, C. *Angew. Chem., Int. Ed.* **2004**, *43*, 2959−2962.
(2) Shimizu, T.; Kogiso, M.; Masuda, M. *J. Am. Chem. Soc.* **1997**, *119*, 6209−6210.
(3) Trager, O.; Sowade, S.; Bottcher, C.; Fuhrhop, J. H. *J. Am. Chem. Soc.* **1997**, *119*, 9120−9124.
(4) Hartgerink, J. D.; Beniash, E.; Stupp, S. I. *Science (Washington, DC, U.S.)* **2001**, *294*, 1684−1688.
(5) Kerckhoffs, J. M. C. A.; van Leeuwen, F. W. R.; Spek, A. L.; Kooijman, H.; Crego-Calama, M.; Reinhoudt, D. N. *Angew. Chem., Int. Ed.* **2003**, *42*, 5717−5722.
(6) Lee, M.; Lee, S. J.; Jiang, L. H. *J. Am. Chem. Soc.* **2004**, *126*, 12724−12725.
(7) Percec, V.; Glodde, M.; Bera, T. K.; Miura, Y.; Shiyanovskaya, I.; Singer, K. D.; Balagurusamy, V. S. K.; Heiney, P. A.; Schnell, I.; Rapp, A.; Spiess, H. W.; Hudson, S. D.; Duan, H. *Nature (London, U.K.)* **2002**, *419*, 862.
(8) Pollard, T. D. *Nature (London, U.K.)* **2003**, *422*, 741−745.
(9) Whitesides, G. M.; Grzybowski, B. *Science (Washington, DC, U.S.)* **2002**, *295*, 2418−2421.
(10) Newkome, G. R.; Baker, G. R.; Saunders, M. J.; Russo, P. S.; Gupta, V. K.; Yao, Z. Q.; Miller, J. E.; Bouillion, K. *J. Chem. Soc., Chem. Commun.* **1986**, 752−753.
(11) Newkome, G. R.; Yao, Z. Q.; Baker, G. R.; Gupta, V. K.; Russo, P. S.; Saunders, M. J. *J. Am. Chem. Soc.* **1986**, *108*, 849−850.
(12) Newkome, G. R.; Baker, G. R.; Arai, S.; Saunders, M. J.; Russo, P. S.; Theriot, K. J.; Moorefield, C. N.; Rogers, L. E.; Miller, J. E.; Lieux, T. R.; Murray, M. E.; Phillips, B.; Pascal, L. *J. Am. Chem. Soc.* **1990**, *112*, 8458−8465.
(13) Joester, D.; Losson, M.; Pugin, R.; Heinzelmann, H.; Walter, E.; Merkle, H. P.; Diederich, F. *Angew. Chem., Int. Ed.* **2003**, *42*, 1486−1490.
(14) Schenning, A. P. H. J.; Elissen-Roman, C.; Weener, J. W.; Baars, M. W. P. L.; van der Gaast, S. J.; Meijer, E. W. *J. Am. Chem. Soc.* **1998**, *120*, 8199−8208.

10.1021/la7021177 CCC: $40.75
Published on Web 01/19/2008

Scheme 1. Procedure for the Synthesis of the One-Directional Arborol, [9]-10

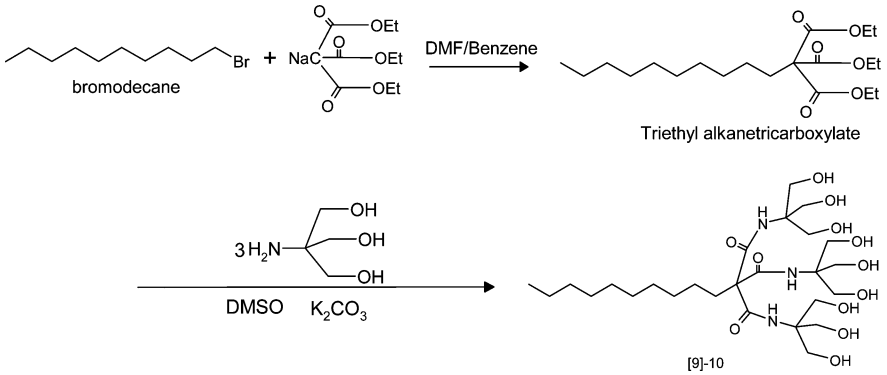

concentrated in vacuo, and dried in a high vacuum oven at 40 °C overnight to afford (95%) the desired product.

$n = 6$: ^{1}H NMR (300 MHz, $CDCl_3$): $\delta = 0.84$ [t, C**H**$_3$, 3H], 1.22−2.00 [m, (C**H**$_2$)$_5$, -OCH$_2$C**H**$_3$, 19H], 4.25 (q, OC**H**$_2$CH$_3$, 6H); ^{13}C NMR $\delta = 13.7$ (**C**H$_3$), 22.2−33.0 (**C**H$_2$), 62.0 (**C**-O), 65.3 (**C**-C═O), and 166.8 (**C**═O). $n = 8$: ^{1}H NMR (300 MHz, $CDCl_3$): $\delta = 0.84$ [t, C**H**$_3$, 3H], 1.22−2.00 [m, (C**H**$_2$)$_5$, -OCH$_2$C**H**$_3$, 23H], 4.25 (q, OC**H**$_2$CH$_3$, 6H); ^{13}C NMR $\delta = 13.7$ (**C**H$_3$), 23.0−33.7 (**C**H$_2$), 62.3 (**C**-O), 66.0 (**C**−C═O), and 167.5 (**C**═O). $n = 10$: ^{1}H NMR (300 MHz, $CDCl_3$): $\delta = 0.84$ [t, C**H**$_3$, 3H], 1.22−2.00 [m, (C**H**$_2$)$_5$, OCH$_2$C**H**$_3$, 27H], 4.25 (q, OC**H**$_2$CH$_3$, 6H); ^{13}C NMR $\delta = 14.0$ (**C**H$_3$), 22.5−33.2 (**C**H$_2$), 61.8 (**C**-O), 65.5 (**C**−C═O), and 167.0 (**C**═O).

These data confirm the structural composition and match the original data.

One-Directional Arborols. General Amide Formation. The previous ester (2.0 mmol) and tris(hydroxymethyl)aminomethane (6 mmol) were dissolved in DMSO (10 mL) and stirred over K_2CO_3 overnight at room temperature. The mixture was filtered and poured into water to yield a precipitate, centrifuged to isolate the solid, which was washed with water twice, and dried in vacuo at 40 °C overnight, to yield 80%. $n = 6$: ^{1}H NMR (300 MHz, *d*-DMSO): $\delta = 0.86$ [t, C**H**$_3$, 3H], 1.23−2.00 [m, (C**H**$_2$)$_5$, 10H], 3.53 (d, HOC**H**$_2$, 12H), 4.00−7.00 (m, O**H**, N**H**); ^{13}C NMR $\delta = 13.9$ (**C**H$_3$), 22.0−31.1 (**C**H$_2$), 54.0 (**C**-N), 60.3 (**C**-O), 62.1 (**C**−C═O), and 171.0 (**C**═O). $n = 8$: ^{1}H NMR (300 MHz, *d*-DMSO): $\delta = 0.86$ [t, C**H**$_3$, 3H], 1.23−2.00 [m, (C**H**$_2$)$_5$, 14H], 3.53 (d, HOC**H**$_2$, 12H), 4.68 (t, O**H**), 7.45 (s, N**H**); ^{13}C NMR $\delta = 14.0$ (**C**H$_3$), 22.1−31.3 (**C**H$_2$), 53.6 (**C**-N), 60.3 (**C**-O), 62.1 (**C**−C═O), and 171.0 (**C**═O). $n = 10$: ^{1}H NMR (300 MHz, *d*-DMSO): $\delta = 0.88$ [t, C**H**$_3$, 3H], 1.23−2.00 [m, (C**H**$_2$)$_5$, 18H], 3.53 (d, HOC**H**$_2$, 12H), 4.70 (t, O**H**), 7.46 (s, N**H**);^{13}C NMR $\delta = 14.0$ (**C**H$_3$), 22.1−31.3 (**C**H$_2$), 53.6 (**C**-N), 60.3 (**C**-O), 62.1 (**C**−C═O), and 171.0 (**C**═O).

These spectra confirmed the formation of the original compounds.

Surface Pressure Measurements. The pressure versus area isotherms of [9]-10 and [9]-8 were measured. The trough was first wiped with Kimwipes paper soaked in $CHCl_3$ followed by EtOH. After the surface was clean and dry, the trough was filled with dust-free, deionized water from a Barnstead Nanopure water purification system. [9]-8 or [9]-10 was dissolved in MeOH and diluted with $CHCl_3$ (vol ratio MeOH/$CHCl_3$ was 1:9) to yield a 1 mg/mL solution, which was spread on the water surface drop-by-drop from a minimum height (about 1 mm). The carrier solvent was allowed to evaporate for 30 min, and then the barriers were closed at a rate of 150 cm^2/min. Three different amounts (600, 700, and 800 μg) of solution were studied repeatedly at several compressions. In addition to the conventional drop-by-drop method, a calibrated atomizer was used as an alternate way to deliver molecules to the surface by spraying.

Brewster Angle Microscopy (BAM). A home-built Brewster angle microscope was mounted on a NIMA Langmuir trough (NIMA Technology Model 312 D), equipped with a CCD camera (FastCam super 10K with Kodak Motion Corder analyzer Ps-220, Video Kommunikation GMBH) as the video recorder with a frequency of 30 frames/s. The laser beam (wavelength of 514 nm, Innova 90 C, Coherent) for the BAM was operated at a power of 60 mW to give sufficient light intensity for recording. One-directional arborol [9]-8 was dissolved in MeOH at a concentration of 10 mg/mL, and the solution was diluted with $CHCl_3$ to a concentration of 1 mg/mL. In the Langmuir trough, 200 μL of this solution was spread onto the subphase consisting of deionized water (NANOpure Diamond, Barnstead, 18.2 MΩ) using a syringe. After that, the Langmuir trough was left undisturbed for 30 min to ensure solvent evaporation. Experiments were performed at 22 ± 1 °C. After solvent evaporation, the mechanical barriers were once closed to a calculated 1 Å^2/molecule and opened to a calculated 4 Å^2/molecule at a constant speed of 50 cm^2/min. These small molecular areas were selected to investigate possible surface structures. Scanning of the focus area was performed to obtain the entire image in focus; a network-like structure of adsorbed arborols was seen throughout the air−water interface when the barriers were open.

Transmission Electron Microscopy. Images were collected on a JEM-100CX (JEOL, Ltd.) in the conventional transmission mode using 80 keV. The samples were dropped on a carbon coated copper grid (Cat # CF 400-CO) and stained by uranyl acetate.

Atomic Force Microscopy. The experiments were conducted on a Digital Instruments Nanoscope III multimode SPM in tapping mode. The tip was a silicon nitride probe from Digital Instruments, type NP-S. The samples were Langmuir−Blodgett films of [9]-8 on mica. To prepare the films, the freshly cleaved mica was dipped in the well of the Langmuir−Blodgett trough before [9]-8 solutions were applied on the water surface. The surface pressure was set at 25 mN/m. At this value, [9]-8 was roughly in a 2D-solid state at the air−water interface. When the surface pressure reached this value, the mica was withdrawn while the surface pressure was held to be stable at 25 mN/m.

Results and Discussion

Solubility and Surface Tensiometry. All the arborols are more soluble in MeOH than they are in water. The solubility of one-directional arborols in water decreases dramatically with increasing length of the alkane focal group, from 13.0 mmol/L ($n = 6$) to 1.4 mmol/L ($n = 8$) or even less considering the possibility for supersaturation. The solubility of [9]-10 is less than 0.017 mmol/L (0.01 mg/mL).

The surface tensions of [9]-6 solutions were measured by the Wilhelmy plate method with a Nima sensor, type PS4 in a 5 mL Teflon vial at 25 °C. The surface tension decreased with concentration (Figure 1), reaching a plateau above the cmc of 8.8 mmol/L (4.7 mg/mL).

The surface tension for [9]-8 solutions was measured by working from low to high concentrations. The weighed solid [9]-8 was added to water, and the mixture was heated to 80 °C, then sonicated for 3−6 min (depending on the concentration) in a 30 °C water bath. The solutions were stored at 25 °C and measured 20 min after they reached apparent uniformity. Each concentration was checked five times at 25 °C. At concentrations

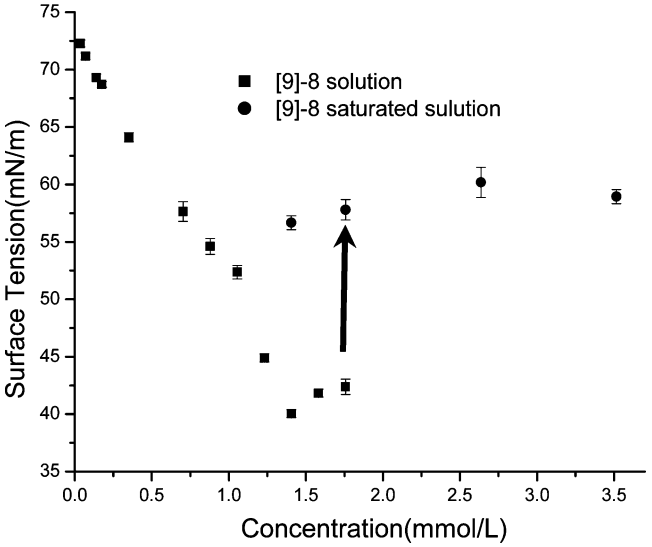

Figure 2. Surface tension of [9]-8 at different concentrations. Squares represent [9]-8 solutions without solid precipitation. Circles represent [9]-8 saturated solutions with solid precipitation. The arrow indicates the increased surface tension after the solute precipitated.

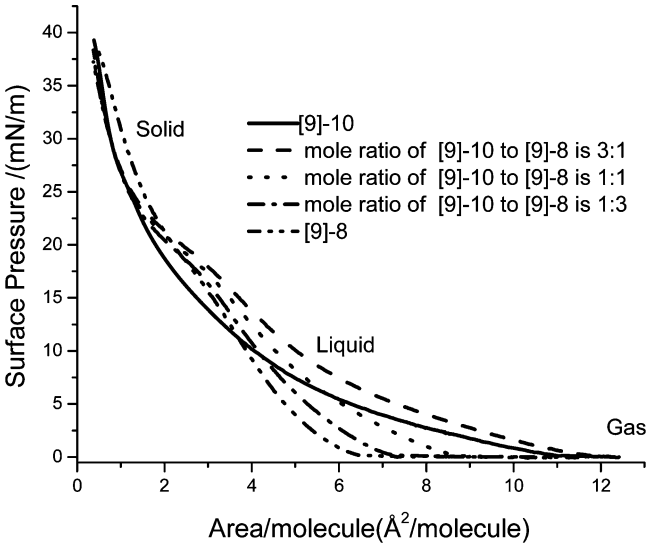

Figure 3. Surface pressure and area isotherm of [9]-8, [9]-10, and their mixtures at indicated mole ratios, first compression.

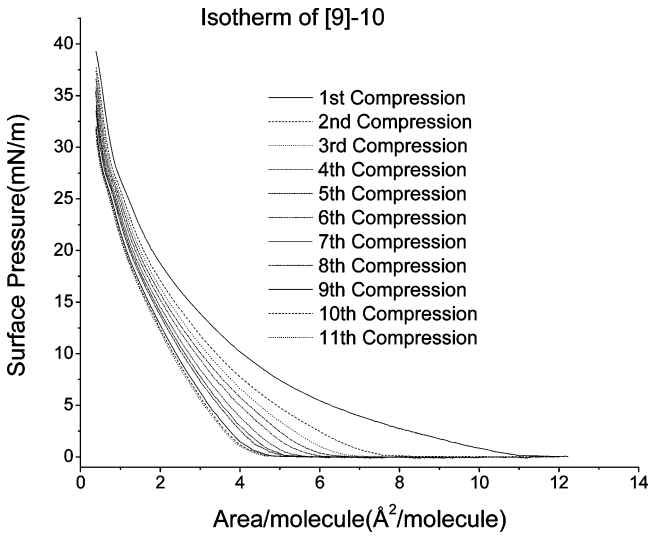

Figure 4. Surface pressure and area isotherm of [9]-10 with 11 compressions. Each isotherm of the total 11 compressions is listed.

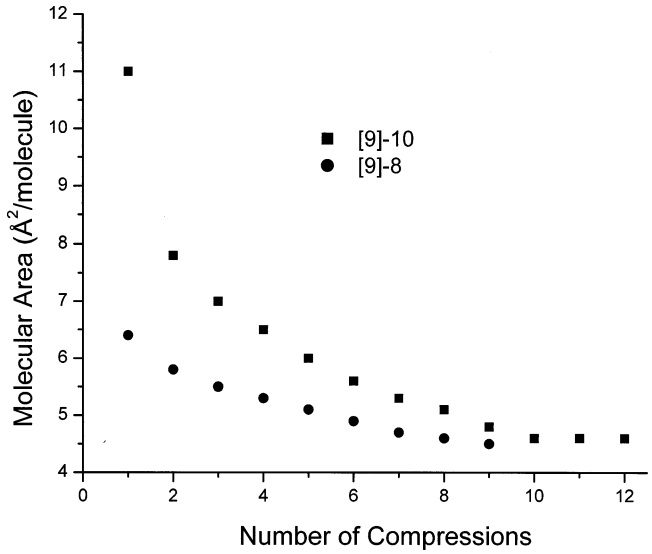

Figure 5. Starting areas of the liquid phase for isotherms of [9]-10 and [9]-8 at different compressions. In the gas phase, which is flat in the isotherm, the surface pressure is 0−0.1 mN/m. The starting area of the liquid phase is identified graphically as the area where the surface pressure begins to increase on compression.

up to 1.76 mmol/L (1 mg/mL), there was no solid precipitation during the measurement. At higher concentrations, 2.6 and 3.5 mmol/L (1.5 and 2.0 mg/mL, respectively), precipitation was observed even before the surface pressure experiments could be completed. After being stored overnight, solids had precipitated from all solutions with concentrations exceeding 1.4 mmol/L (800 μg/mL). When the surface tension of the precipitate-containing sample was measured, a dramatic increase of surface tension was found when compared to the earlier measurements prior to precipitation, as shown in Figure 2 labeled by the arrow. According to the observed linear relation of the surface pressure and concentration in dilute solution, the saturated composition on the previous day was ca. 700 μmol/L (400 μg/mL).

Surface Pressure Isotherms of Pure One-Directional Surfactants. The solubilities of [9]-8 and [9]-10 in water are low enough to permit the measurement of meaningful surface pressure−area isotherms (Figure 3). The compression was repeated 9 times for [9]-8 and 11 times for [9]-10. Different volumes of solutions (700 and 600 μL) were loaded on the surface; the isotherms were identical. These large volumes are necessitated by the low solubility of the molecules in volatile solvents and in moderately polar solvents at room temperature. As an alternative to drop-by-drop addition, which might disturb the surface too much, fresh solutions were sprayed onto the Langmuir trough using a calibrated atomizer. This yielded similar results.

In the surface pressure−area isotherm of [9]-8, at least three phases can be recognized; these are the 2-D gas, liquid, and solid. In the isotherm of [9]-10, the 2-D gas phase is easily identified, but it is difficult to distinguish the liquid and solid phases.

One thing in common for these two arborols is the shifting of the isotherm to the left (i.e., toward smaller molecular areas) as repeated compressions are applied (Figures 4 and 5). Another common feature is that a stable isotherm is reached after multiple compressions (nine to 11). To understand this phenomenon, an experiment was conducted on [9]-10 after 11 compressions. The barriers were held open for 30 min and compressed one more time. The isotherm was identical to the one obtained on the 11th compression; there was no shifting back to the larger molecular area. Thirty minutes of relaxation time is sufficient for regular

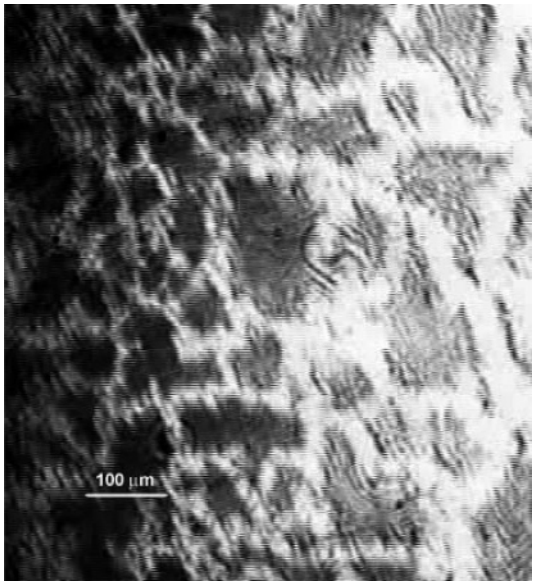

Figure 6. Structure of the [9]-8 arborol at the air−water interface as observed with Brewster angle microscopy. The image is captured from a movie of the one-directional arborol at the interface. The surface tension was 20 mN/m.

amphiphiles to spread out from the solid state to the gas state. This suggests that a permanent change of the arrangement of the arborols on the surface may have occurred during consecutive compression−expansion cycles.

Another feature common to both [9]-8 and [9]-10 isotherms is the small molecular areas, evident even on the first compression (Figures 3 and 4). Considering the large hydrophilic canopy of the tree-shaped molecules, subsurface aggregation is a possibility. Perhaps the molecules form micellar or oligomeric structures and submerge in the substrate, which would permanently change the arborol content on the surface. As shown in Figure 5, the trend of the starting area is downward with each compression, but a minimum value is reached after ca. nine repeated compressions. This indicates that any changes to the surface content or morphology are limited and that a stable state is reached eventually. No particles were found in the subphase, as checked by light scattering, but net-like structures of the aggregates on the surface were detected by BAM (see Figure 6). These structures remained unchanged as long as a constant surface pressure was maintained. Watching the network structure over a period of 15 min, no discernible changes of the pattern at the interface were noticed. Submersion of the one-directional arborols cannot be ruled out, but their participation in surface structures is certain. Not all the arborols were found in the structures, however. AFM images of the films deposited on mica show what seem to be patches of a [9]-8 monolayer, judging by the height and area measurement of bumps in the AFM images (Figure 7). The average height of these bumps was 1.37 ± 0.01 nm, which is very close to the calculated length of one single [9]-8 from ChemDraw (1.6 nm); the average area of these bumps was 45.5 ± 27.0 nm^2, which is much larger than the area occupied by one [9]-8 molecule. The area measurement was carried out on 700 bumps in the range of 12.5−300.0 nm^2 using ImagePro. Reasons to choose this range are that the area below 12.5 nm^2 is difficult to separate from noise and that no bump larger than 170 nm^2 is found.

Evidence for Self-Assembly. At bulk concentrations exceeding the cmc, aggregates are expected (even if no structures were detectable in the subphase after surface layer spreading, as noted previously). A TEM image of a 7% [9]-6 arborol preparation

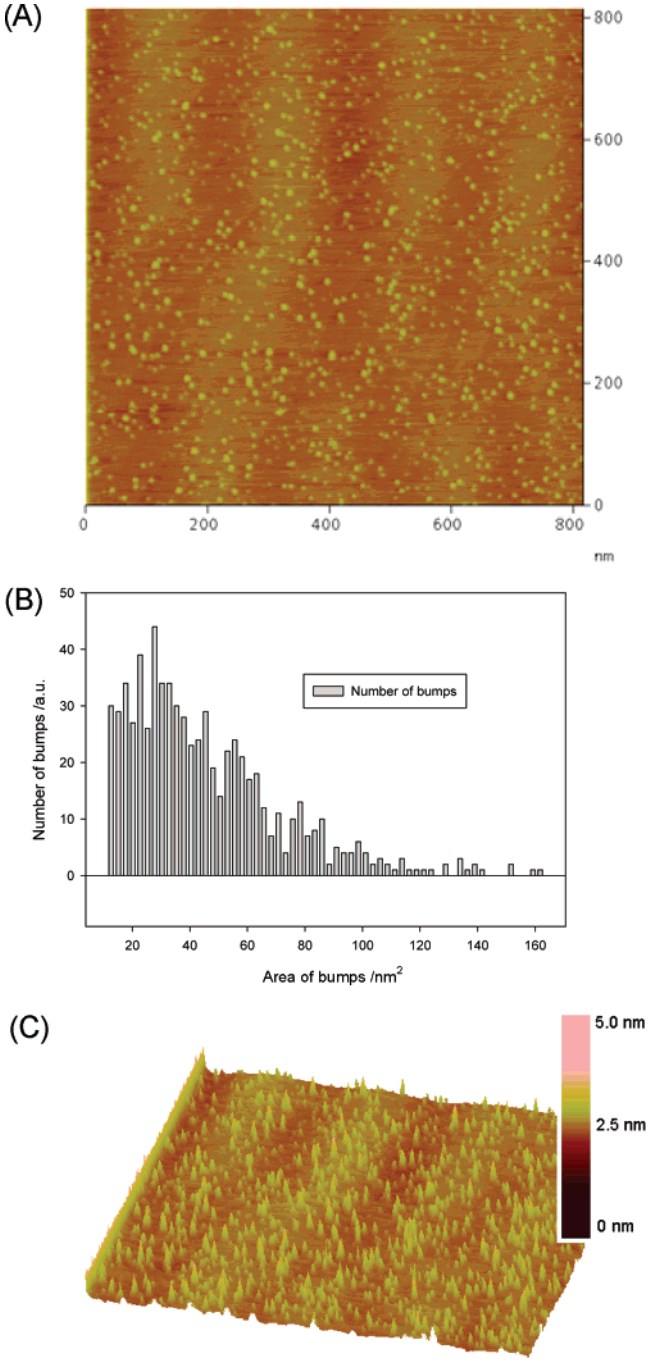

Figure 7. AFM image of the [9]-8 monolayer on mica. The sample was prepared using a NIMA Langmuir−Blodgett trough at a surface tension of 25 mN/m. The average height of these bumps was 1.37 nm. (A) 2-D view of [9]-8 on mica by AFM; (B) area measurement of 700 bumps in the search range of 12.5−300.0 nm^2; and (C) 3-D view of the same area.

indicates the existence of aggregates (inset of Figure 8) with a wide size distribution.

The same [9]-6 solution was checked by multiple-angle dynamic light scattering after filtering with 0.45 μm Millex HV PVDF membranes. A hydrodynamic radius of 282 ± 13 nm was derived from a linear fit of decay rate versus squared scattering vector magnitude. An inverse Laplace transformation algorithm (CONTIN[13]) applied to the DLS data measured at a scattering angle of 90° revealed a single broad peak, apart from a small peak at very large sizes (exceeding that of the filter), which probably reflects baseline anomalies or number fluctuations (Figure 8). The main single peak reflects the wide size distribution

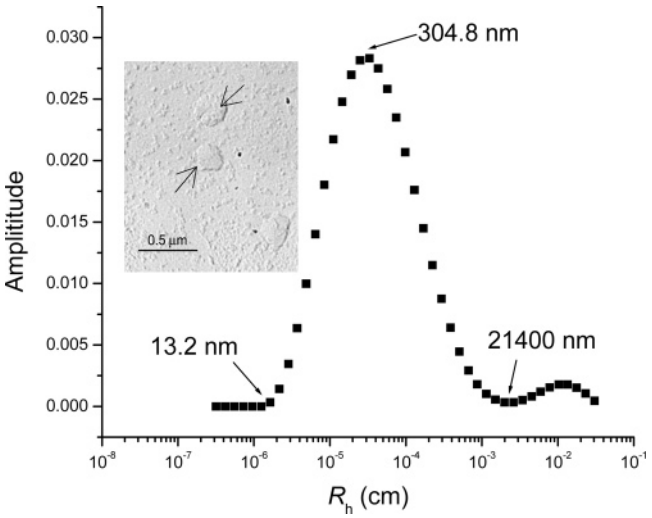

Figure 8. Distribution of scattering amplitudes chosen by the inverse Laplace transform program CONTIN for 7 mg/mL [9]-6 solution reflects the wide size distribution of the aggregates. Inset: TEM image of 7% [9]-6 solution; the arrows indicate large micelles or structures.

of the aggregates. It is not known whether smaller structures coexist with the large ones.

Conclusion

To summarize, one-directional arborols are effective surface-active agents. The surface properties change dramatically as the carbon number *n* increases from 6 to 8 to 10, but surface activity is evident even for the shortest aliphatic chain tested. Surface pressure isotherms, performed repetitively, and BAM observations indicate that structures exist at the air−water interface after successive compressions. Large structures are found in [9]-6 solutions, which is not yet fully understood. One possibility is that the hydrophobic tail extends outward to stabilize a bilayer of comparatively low hydrophobic content, which might prove to be useful for the storage of semipolar molecules. Future research and development on these materials may profitably concentrate on interactions with other large structures. For example, amphiphilic arborols may be useful in situations where it is desirable to tailor colloidal particle or liposome surface character. An area ripe for investigation is the ability of these one-directional arborols to limit fibril formation, especially the very long fibrils formed by hydrogel-forming two-directional arborols (e.g., [9]-*n*-[9]).[12,15]

Acknowledgment. This work was supported by NSF-DMR-0075810 (P.S.R.) and NSF-DMR-041780, NSF-INT-0405242, and AFOSR-F49620-02-1-0428,2 (G.R.N.). D.D. acknowledges the support of an IGERT Fellowship (NSF-DGE-9987603). We express our thanks to Dr. Thomas Fischer of Florida State University for assistance with Brewster angle microscopy.

LA7021177

(15) Yu, K. H.; Russo, P. S.; Younger, L.; Henk, W. G.; Newkome, G. R.; Baker, G. *J. Polym. Sci., Part B: Polym. Phys.* **1997**, *35*, 2787−2793.